Available online at www.sciencedirect.com
SCIENCE DIRECT®
Journal of Solid State Chemistry 178 (2005) 1221–1229
JOURNAL OF SOLID STATE CHEMISTRY
www.elsevier.com/locate/jssc

Structures, magnetic, and thermal properties of Ln_3MoO_7 (Ln = La, Pr, Nd, Sm, and Eu)

Hiroaki Nishimine, Makoto Wakeshima, Yukio Hinatsu*

Division of Chemistry, Graduate School of Science, Hokkaido University, Sapporo 060-0810, Japan

Received 18 August 2004; received in revised form 7 October 2004; accepted 8 October 2004

Abstract

Ternary lanthanide–molybdenum oxides Ln_3MoO_7 (Ln = La, Pr, Nd, Sm, Eu) have been prepared. Their structures were determined by X-ray diffraction measurements. They crystallize in a superstructure of cubic fluorite and the space group is $P2_12_12_1$. The Mo ion is octahedrally coordinated by six oxygens and the slightly distorted octahedra share corners forming a zig-zag chain parallel to the b-axis. These compounds have been characterized by magnetic susceptibility and specific heat measurements. The La_3MoO_7 shows complex magnetic behavior at 150 and 380 K. Below these temperatures, there is a large difference in the temperature-dependence of the magnetic susceptibility measured under zero-field-cooled condition and under field-cooled condition. The Nd_3MoO_7 show a clear antiferromagnetic transition at 2.5 K. From the susceptibility measurements, both Pr_3MoO_7 and Sm_3MoO_7 show the existence of magnetic anomaly at 8.0 and 2.5 K, respectively. The results of the specific heat measurements also show anomalies at the corresponding magnetic transition temperatures. The differential scanning calorimetry measurements indicate that two phase-transitions occur for any Ln_3MoO_7 compound in the temperature range between 370 and 710 K.

Keywords: Magnetic properties; Lanthanide; Molybdenum; Oxide; Magnetic susceptibility; Specific heat; Antiferromagnetic transition; Structural phase transition; Differential scanning calorimetry

1. Introduction

The solid state chemistry of mixed metal oxides containing both lanthanides and 4*d* or 5*d* transition metals has attracted a great deal of interest. In recent years, compounds of composition Ln_3MO_7, where Ln is a lanthanide and M is the 4*d* or 5*d* transition metal, have been investigated by many researchers [1–23]. In 1979, Rossell et al. determined the crystal structures of Y_3TaO_7 and Y_2GdSbO_7 [1,2]. The structures are basically similar. One-third of the Ln cation are 8-coordinated and lie in [001] rows which alternate with parallel rows of corner-linked MO_6 coordination octahedra within slabs parallel to [100]. The remaining Ln cations lie between these slabs in seven-fold coordination. A variety of the space groups such as *Pnma*, *Cmcm*, $P2_12_12_1$, and $C222_1$ have been proposed for the Ln_3MO_7. For the Ln_3RuO_7 (Ln = La, Pr, Nd, Sm–Gd) [3,4,10–17], Ln_3IrO_7 (Ln = Pr, Nd, Sm, Eu) [6,7,21], and Ln_3ReO_7 (Ln = Pr, Nd, Sm–Tb) [8,19,23], *Cmcm* appears to provide a good description, while for Ln_3NbO_7 (Ln = La) [7] and Ln_3MoO_7 (Ln = La, Pr) [9,20], *Pnma* and $P2_12_12_1$ have been adopted, respectively.

As for the Mo compounds, Prevost-Czeskleba first reported that Ln_3MoO_7 (Ln = La, Pr, Nd, Sm, Eu) crystallized in an orthorhombic phase with space group *Cmcm* from their powder X-ray diffraction measurements [5]. Later, Greedan et al. [9] and Barrier and Gougen [20] prepared single crystals of Ln_3MoO_7 (Ln = La, Pr) and performed their single crystal X-ray diffraction measurements. Their experimental results show that these Ln_3MoO_7 compounds crystallize in the orthorhombic space group $P2_12_12_1$.

*Corresponding author. Fax: +81 11 706 2702.
E-mail address: hinatsu@sci.hokudai.ac.jp (Y. Hinatsu).

0022-4596/$ - see front matter © 2004 Elsevier Inc. All rights reserved.
doi:10.1016/j.jssc.2004.10.013

Greedan et al. studied the electronic and thermal properties of La_3MoO_7 by magnetic susceptibility, electric resistivity, and neutron diffraction measurements [9]. The magnetic susceptibility was quite complex. The main feature was the existence of a broad maximum at 655 K, which was interpreted as due to intrachain spin correlations of the Mo^{5+} ions. Several other anomalies were observed at 483, 140, and 100 K. There was an indication from neutron diffraction data for the onset of long-range antiferromagnetic order below 100 K. Differential scanning calorimetry (DSC) data showed that the anomalies at 373 and 483 K may be due to the phase transitions. However, magnetic and thermal studies on other Ln_3MoO_7 compounds except for La_3MoO_7 have not been performed yet.

Compounds of composition Ln_3MO_7 have, in general, quasi-one-dimensional feature in their crystal structures. Therefore, we can expect to observe peculiar magnetic and electronic properties reflecting this low-dimensional feature. In the present study, we have prepared a series of Ln_3MoO_7 compounds (Ln = La, Pr, Nd, Sm, Eu). Through X-ray diffraction measurements, their crystal structures have been determined. The magnetic susceptibility and specific heat measurements have been performed from 1.8 K to room temperature.

2. Experimental

2.1. Sample preparation

As starting materials, Ln_2O_3, MoO_2, and MoO_3 were used. For the preparation of Ln = Pr compound, Pr_6O_{11} was used as a starting material. To obtain praseodymium sesquioxide Pr_2O_3, the Pr_6O_{11} was reduced in a flowing H_2 atmosphere at 900 °C for a day. They were weighed in an appropriate metal ratio and were ground in an agate mortar. The mixtures were pressed into pellets and then sealed in an evacuated platinum tube. They were heated at 1200 °C for 12 h, and then cooled down to room temperature. After regrinding and repelleting, the same heating procedure was repeated again.

2.2. X-ray diffraction analysis

Powder X-ray diffraction (XRD) measurements were carried out in the region of $10° \leqslant 2\theta \leqslant 120°$ using Cu$K\alpha$ radiation on a Rigaku MultiFlex diffractometer equipped with a curved graphite monochromator. The structures were refined with the Rietveld method. For La_3MoO_7, the XRD profiles were obtained in the temperature range from 300 to 500 K. The Rietveld analyses were carried out with the program RIETAN 2000 [24] using collected diffraction data.

2.3. Magnetic susceptibility measurements

The temperature-dependence of the magnetic susceptibility was measured in an applied field of 0.1 T over the temperature range of $1.8\,K \leqslant T \leqslant 300\,K$, using a SQUID magnetometer (Quantum Design, MPMS5S). The susceptibility measurements were performed either using zero field cooling (ZFC) and field cooling (FC) conditions. The former was measured upon heating the sample to 300 K under the applied magnetic field of 0.1 T after zero-field cooling to 1.8 K. The latter was measured upon cooling the sample from 300 to 1.8 K at 0.1 T.

2.4. Specific heat measurements

Specific heat measurements were performed using a relaxation technique by a commercial heat capacity measuring system (Quantum Design, PPMS) in the temperature range of 1.8–300 K. The sintered sample in the form of a pellet was mounted on a thin alumina plate with Apiezon for better thermal contact.

2.5. Differential scanning calorimetry measurements

The DSC measurements were carried out under flowing Ar gas atmosphere over the temperature range of 300–800 K using DSC 200 (Seiko, Japan). The heating rate was 5 K/min.

3. Results and discussion

3.1. Preparation and crystal structure

We have successfully prepared a series of compounds Ln_3MoO_7 (Ln = La, Pr, Nd, Sm, Eu) in evacuated platinum tubes heated at 1200 °C for 12–24 h. Fig. 1 shows the powder X-ray diffraction profile for Nd_3MoO_7 measured at room temperature, as an example. The powder X-ray diffraction profiles for Ln_3MoO_7 (Ln = La, Pr) are quite similar to those reported earlier [9,20]. Their crystal structures have been elucidated and they are orthorhombic with space group $P2_12_12_1$ (No. 19). We have performed refinements of the crystal structures for other Ln_3MoO_7 (Ln = Nd, Sm, Eu) with the same space group $P2_12_12_1$. The lattice parameters and reliability factors R for Ln_3MoO_7 (Ln = La, Pr, Nd, Sm, Eu) are listed in Table 1. Table 2 lists the crystallographic data for Nd_3MoO_7, as a representative of Ln_3MoO_7 (Ln = La, Pr, Nd, Sm, Eu). The results of the Rietveld analysis show that Ln_3MoO_7 (Ln = Nd, Sm, Eu) are isomorphous with La_3MoO_7 and Pr_3MoO_7. Fig. 2 shows the crystal structure of Nd_3MoO_7. It consists of slabs, parallel to the (a, b) plane, in which rows of corner-linked MoO_6 octahedra

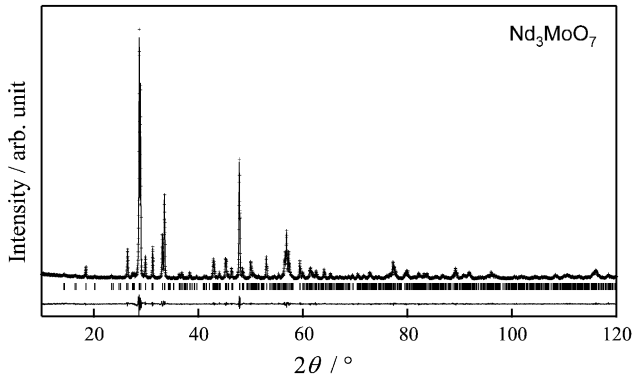

Fig. 1. Powder X-ray diffraction profiles for Nd_3MoO_7. The calculated and observed profiles are shown on the top solid line and cross markers, respectively. The vertical marks in the middle show positions calculated for Bragg reflections. The lower trace is a plot of the difference between calculated and observed intensities.

Table 1
Lattice parameters and reliability factors R for Ln_3MoO_7 (Ln = La, Pr, Nd, Sm, Eu)

Compounds	a (Å)	b (Å)	a (Å)	R_{wp}	R_I
La_3MoO_7	7.599(2)	7.716(2)	11.101(2)	10.71	2.05
Pr_3MoO_7	7.511(2)	7.638(2)	10.892(2)	10.04	2.32
Nd_3MoO_7	7.509(2)	7.605(2)	10.818(2)	10.20	2.08
Sm_3MoO_7	7.451(1)	7.540(1)	10.673(2)	10.58	2.20
Eu_3MoO_7	7.439(2)	7.518(2)	10.623(3)	10.35	1.81

Note: Definition of reliability factors R_{wp} and R_I are given as follows: $R_{wp} = [\Sigma w(|F(o)| - |F(c)|)^2/\Sigma w(|F(o)|^2]^{1/2}$ and $R_1 = \Sigma|I_k(o) - I_k(c)|/\Sigma I_k(o)$.

Table 2
Crystallographic data for Nd_3MoO_7

Atom	Site	x	y	z	B (Å^2)
Space group : $P2_12_12_1$ (No. 19)					
Nd(1)	4a	0.9776(2)	0.0100(4)	0.7545(5)	0.52(5)
Nd(2)	4a	0.7058(4)	0.7545(6)	0.5339(2)	0.46(7)
Nd(3)	4a	0.6936(3)	0.7460(6)	−0.0173(2)	0.17(6)
Mo	4a	0.4968(4)	−0.0011(7)	0.7504(7)	0.20(5)
O(1)	4a	0.569(2)	0.764(4)	0.763(3)	0.9(1)
O(2)	4a	0.798(2)	0.957(4)	0.134(2)	0.9(1)
O(3)	4a	0.117(2)	0.051(4)	0.106(2)	0.9(1)
O(4)	4a	0.820(2)	0.975(4)	0.377(2)	0.9(1)
O(5)	4a	0.204(2)	0.033(4)	0.359(2)	0.9(1)
O(6)	4a	0.954(2)	0.742(5)	−0.112(2)	0.9(1)
O(7)	4a	0.997(3)	0.752(6)	0.620(2)	0.9(1)

$a = 7.509(2)$ Å; $b = 7.605(2)$ Å; $c = 10.818(2)$ Å; $V = 617.8(2)$ Å^3.

running parallel to the b-axis alternate with rows of edge-shared $Nd(1)O_8$ pseudo-cubes. These slabs are separated by Nd(2) and Nd(3) cations which both are seven-coordinated by oxygen atoms.

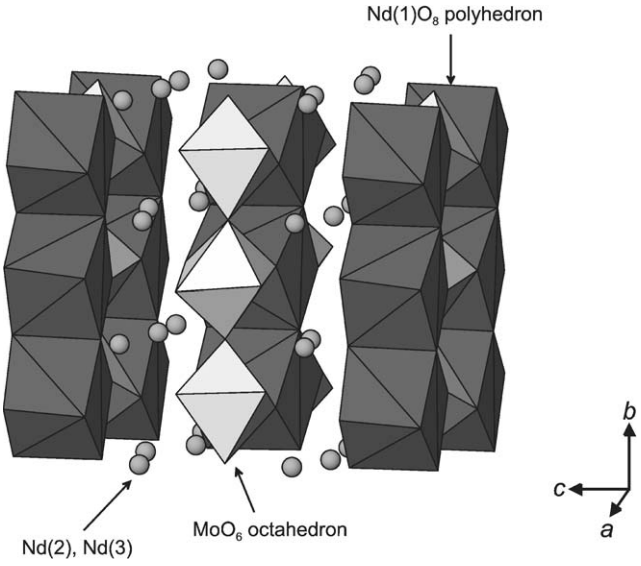

Fig. 2. The crystal structure of Nd_3MoO_7.

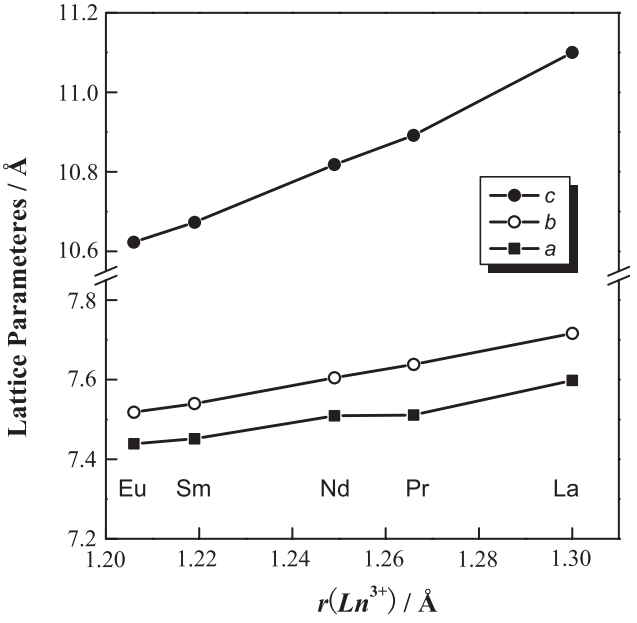

Fig. 3. Variation of lattice parameters for Ln_3MoO_7 (Ln = La, Pr, Nd, Sm, and Eu) with the Ln^{3+} ionic radius in eight coordination.

Fig. 3 shows the variation of lattice parameters for Ln_3MoO_7 with the Ln^{3+} ionic radius in eight coordination. With increasing Ln^{3+} radius, the lattice parameters monotonically increase, which differs from the results for Ln_3IrO_7 (Ln = Pr, Nd, Sm, Eu) [21]. In those iridates, not a monotonical increase of lattice parameters with increasing Ln^{3+} radius has been found and a phase transition of Ln_3IrO_7 has been observed at 262–485 K, i.e., not all the Ln_3IrO_7 compounds have the space group $Cmcm$ at room temperature.

3.2. Magnetic properties

We have performed measurements of the magnetic susceptibility and specific heat in the temperature range of $1.8\,K < T < 400\,K$ and $1.8\,K < T < 300\,K$, respectively.

3.2.1. La_3MoO_7

Figs. 4(a) and (b) show the temperature dependences of the magnetic susceptibility and specific heat for La_3MoO_7, respectively. The variation of the magnetic susceptibility with temperature is complicated. Below 380 K, the divergence between the ZFC and FC susceptibility has been found and the decrease of the susceptibility has been observed when the temperature is decreased through 150 K. This magnetic behavior is quite similar to the magnetic susceptibility data reported by Greedan et al. [9]. However, no anomaly has been observed in the temperature dependence of its specific heat at the corresponding temperature. Greedan et al. also reported that no explanation for the anomaly was available from the neutron diffraction measurements, and that the magnetic behavior observed below 100 K was due to the long-range magnetic orderings of Mo ions [9]. The anomaly observed at 380 K in the magnetic susceptibility is due to a structural phase transition, as will be described later.

3.2.2. Pr_3MoO_7

Figs. 5(a) and (b) show the temperature dependence of the magnetic susceptibility and specific heat for Pr_3MoO_7 from 1.8 to 300 K. The inset figures show their detailed temperature dependence in the low temperature region. The divergence between the ZFC and FC magnetic susceptibility has been observed below 8 K and the increment of the susceptibility with decreasing temperature becomes smaller when the temperature is decreased through this temperature. At the same temperature, this compound shows a broad peak in the specific heat vs. temperature curve (Fig. 5(b)). This behavior indicates that Pr_3MoO_7 has a Schottky-type anomaly [25]. Since the site symmetry of the Pr ion is low in this compound, the ground state of the Pr^{3+} ion should be singlet. Due to a small energy difference between this singlet ground state and the excited state, the Schottky-type specific heat anomaly has been observed [25].

A linear relationship has been observed in the temperature dependence of the inverse magnetic susceptibility between 300 and 400 K. The Curie–Weiss fitting gives the Curie constant (C) and Weiss constant (θ) to be 5.15 (2) emu K/mol and −79 (1) K, respectively. This Curie constant means the effective magnetic moment of Pr_3MoO_7 to be 6.42 μ_B. Three Pr^{3+} ions and one Mo^{5+} ion contribute to the paramagnetism of this compound. Since the theoretical effective magnetic moments of Pr^{3+} and Mo^{5+} ions are 3.58 and 0.87 μ_B, respectively, the expected effective magnetic moment for Pr_3MoO_7 is estimated to be 6.26 μ_B. The experimental value agrees with this estimated moment.

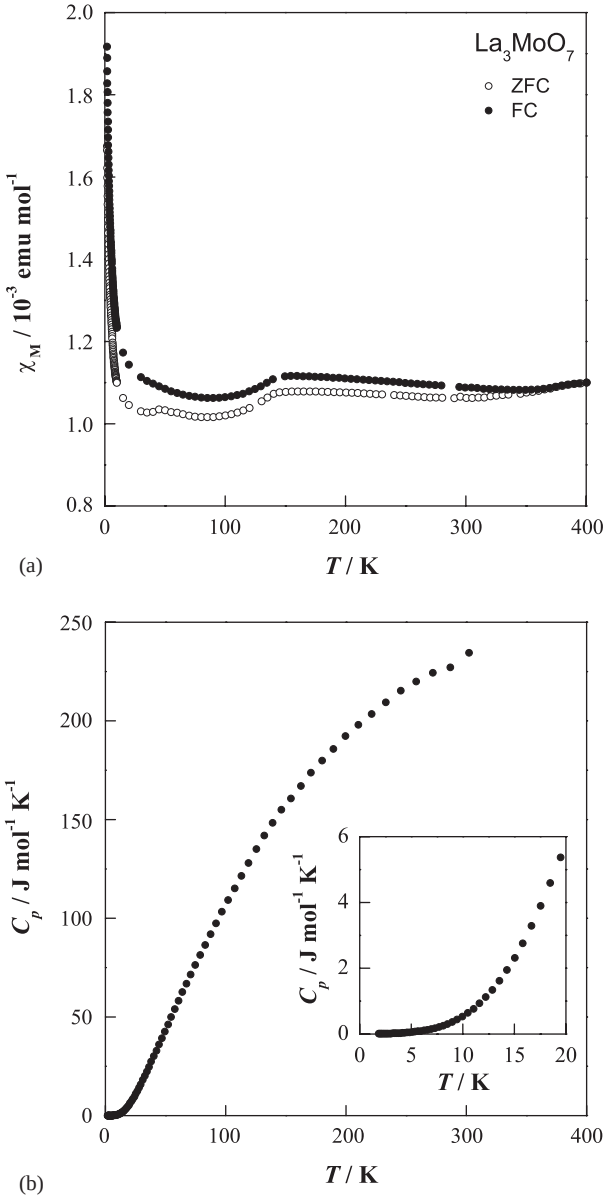

Fig. 4. (a) Temperature dependence of the magnetic susceptibility for La_3MoO_7. (b) Temperature dependence of the specific heat for La_3MoO_7. The inset shows its detailed temperature dependence below 20 K.

3.2.3. Nd_3MoO_7

Fig. 6(a) shows the detailed temperature dependence of the susceptibility for Nd_3MoO_7 below 15 K. It shows a sharp peak at 2.5 K, and when the temperature is furthermore decreased through this temperature, the divergence between the ZFC and FC susceptibilities has been observed. This magnetic behavior is characteristic for the canted antiferromagnetic substance. A λ-type

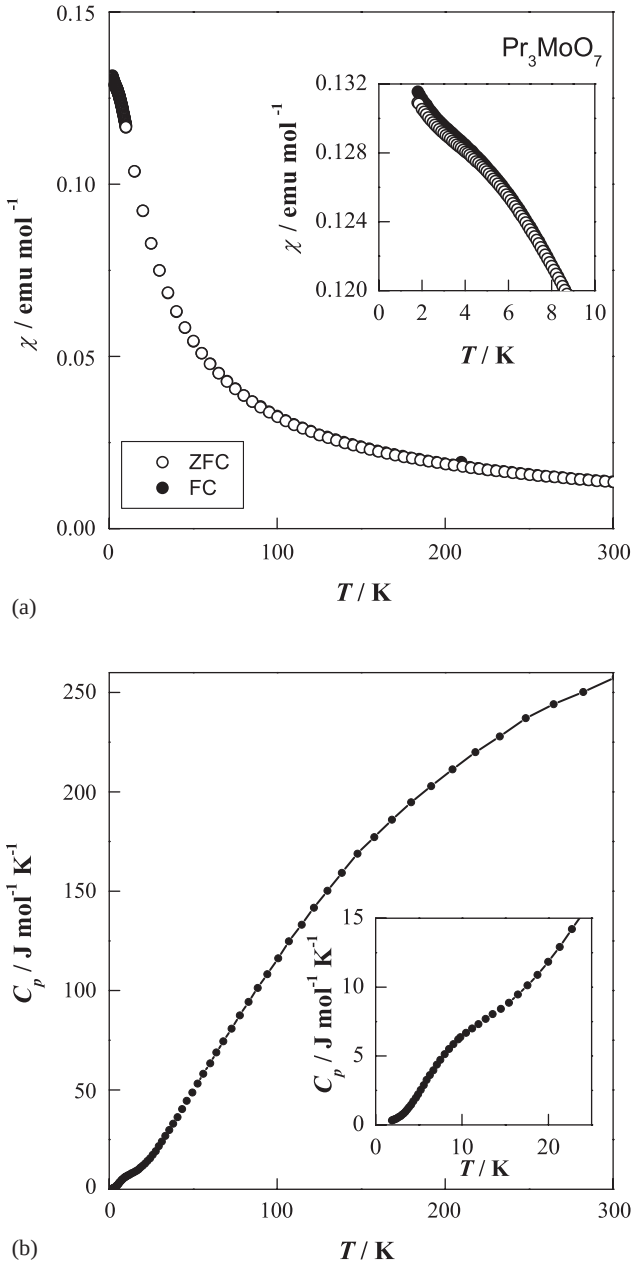

Fig. 5. (a) Temperature dependence of magnetic susceptibility for Pr_3MoO_7. The inset shows its detailed temperature dependence below 10 K. (b) Temperature dependence of the specific heat for Pr_3MoO_7. The inset shows its detailed temperature dependence in low temperature region.

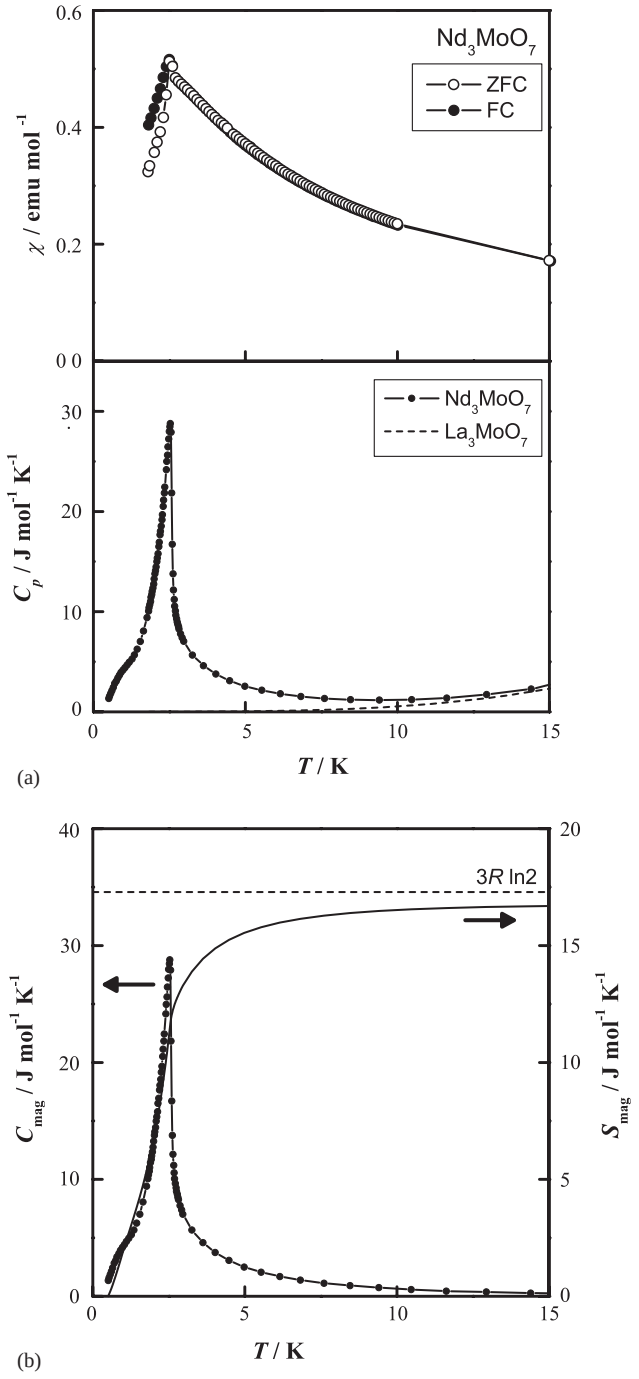

Fig. 6. (a) Temperature dependences of the magnetic susceptibility and specific heat for Nd_3MoO_7 below 15 K. (b) The magnetic specific heat (C_{mag}) and magnetic entropy (S_{mag}) against temperature for Nd_3MoO_7.

specific heat anomaly has been observed at the same temperature.

We will evaluate the magnetic entropy change due to the antiferromagnetic ordering from the data of the specific heat measurements. As shown in Fig. 4(b), the specific heat for La_3MoO_7 shows no magnetic anomaly down to 1.8 K. If we assume that the electronic and lattice contributions to the specific heat are equal between La_3MoO_7 and Nd_3MoO_7, the magnetic specific heat for Nd_3MoO_7 is obtained by subtracting the specific heat of La_3MoO_7 from that of Nd_3MoO_7. From its temperature dependence, the magnetic entropy change associated with the Nd^{3+} antiferromagnetic transition is calculated as shown in Fig. 6(b). It is saturated around 10 K and the magnetic entropy obtained experimentally is about 17.0 J/mol K, which is very close to $3R\ln W = 3R\ln 2 = 17.3$ J/mol K, where

R and W are a molar gas constant and a degree of degeneracy of the ground state, respectively. This result shows that the degeneracy of the ground state should be doublet. Since the low symmetry of the oxygen-coordination around the Nd^{3+} site distorts its crystal electric field, it is expected that the ground state of Nd^{3+} ion should be a Kramers' doublet. That is, the experimental results accords with this expectation.

The Curie–Weiss relationship has been found in the temperature range of $300\,K < T < 400\,K$. The derived fitting constant are $C = 5.22(1)\,emu\,K/mol$ and $\theta = -57.4(8)\,K$. This Curie constant gives the effective magnetic moment of Nd_3MoO_7 to be $6.46\,\mu_B$. Three Nd^{3+} ions and one Mo^{5+} ion contribute to the paramagnetism of this compound. Since the theoretical effective magnetic moments of Nd^{3+} and Mo^{5+} ions are 3.62 and $0.87\,\mu_B$, respectively, the expected effective

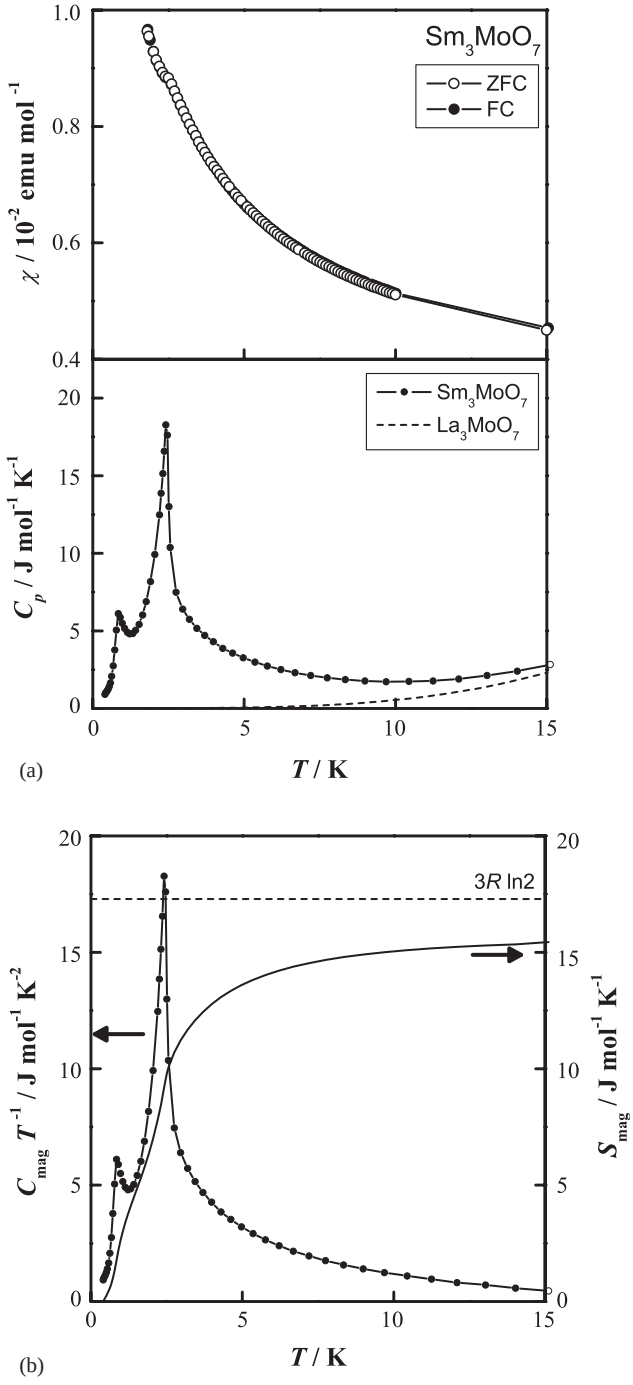

Fig. 7. (a) Temperature dependences of the magnetic susceptibility and specific heat for Sm_3MoO_7 below 15 K. (b) The magnetic specific heat (C_{mag}) and magnetic entropy (S_{mag}) against temperature for Sm_3MoO_7.

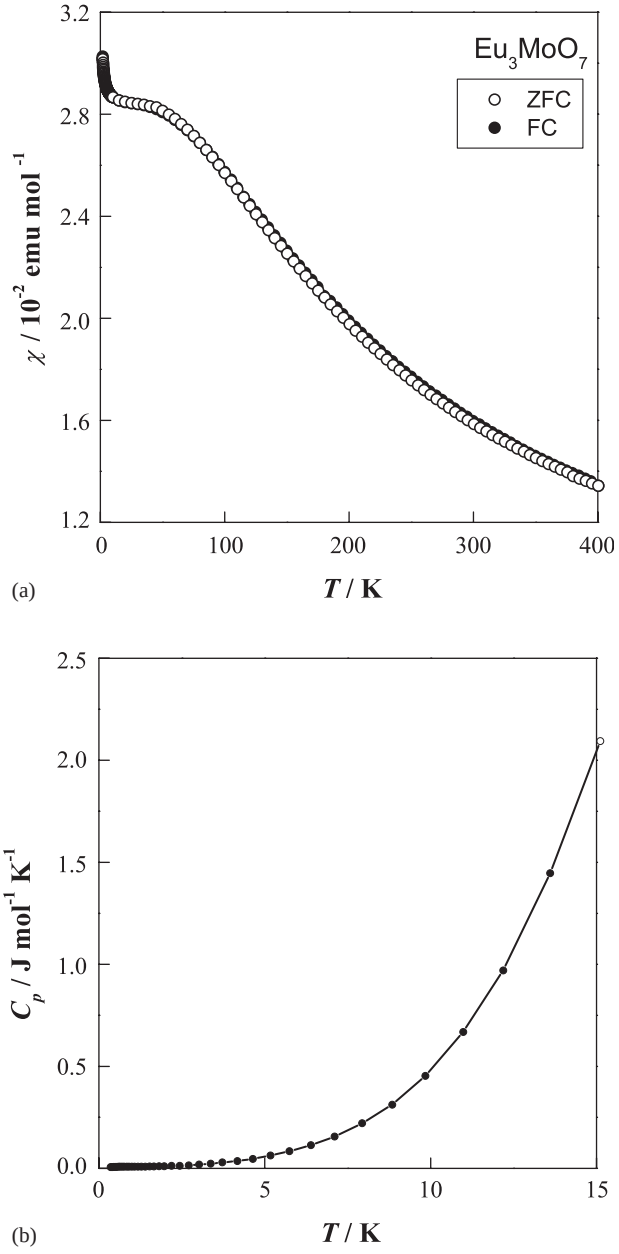

Fig. 8. (a) Temperature dependence of the magnetic susceptibility for Eu_3MoO_7. (b) Temperature dependence of the specific heat for Eu_3MoO_7 at low temperatures.

magnetic moment for Nd_3MoO_7 is estimated to be 6.33 μ_B. The effective magnetic moment obtained from experiment agrees with this estimated value.

3.2.4. Sm_3MoO_7

Fig. 7(a) shows the detailed temperature dependences of the magnetic susceptibility and the specific heat for

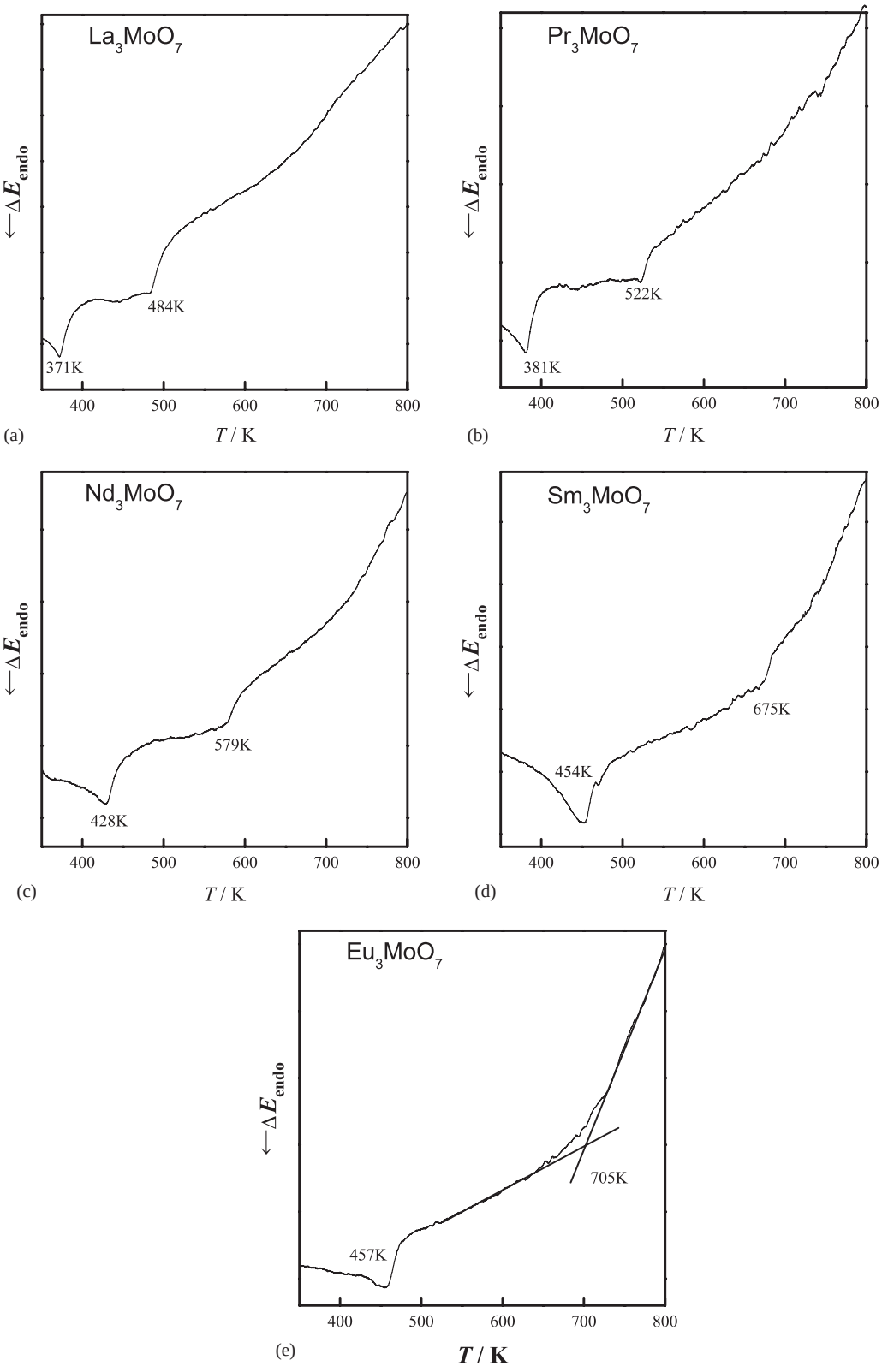

Fig. 9. DSC data for Ln_3MoO_7 (Ln = La, Pr, Nd, Sm, and Eu) during heating in the temperature range of 350–800 K.

Sm_3MoO_7 below 15 K. Measurements of the magnetic susceptibility of Sm_3MoO_7 have been performed in the temperature range of $1.8\,K < T < 400\,K$. No magnetic anomaly has been observed in the high temperature region. A small magnetic anomaly has been found at 2.5 K, but the susceptibility increases with decreasing temperature below this temperature (Fig. 7(a)). A corresponding anomaly has been clearly observed in the specific heat vs. temperature curve. We have performed the specific heat measurements down to 0.4 K using a ^{3}He option for the PPMS equipment. In addition to the anomaly observed at 2.5 K, another λ-type anomaly has been found at 0.8 K (see lower figure of Fig. 7(a)).

In a similar way as the case for Nd_3MoO_7, the magnetic entropy change due to the magnetic transition observed in the Sm_3MoO_7 has been estimated by subtracting the specific heat of La_3MoO_7 from that of Sm_3MoO_7. The results are shown in Fig. 7(b), and the entropy change is estimated to be 15.34 J/mol K, which is close to $3R\ln 2 = 17.29\,J/mol\,K$. This experimental result indicates that the degeneracy of the ground state should be doublet, which accords with the expectation. Low symmetry of the oxygen-coordination around the Sm^{3+} site distorts its crystal electric field and the ground state of the Sm^{3+} ion should be a Kramers' doublet.

In the crystal structure of Sm_3MoO_7, there are two types of oxygen-coordination around Sm sites, one of which is the pseudo-cubic 8-fold coordination and the other is the pentagonal bipyramidal 7-fold coordination. From the results of the specific heat measurements, the existence of the two λ-type anomalies indicates that two kinds of Sm magnetic moments in different coordination environments independently order. At 2.5 K one kind of Sm magnetic moments order antiferromagnetically, and the other kind of Sm magnetic moments are in the paramagnetic state. Therefore, the susceptibility of Sm_3MoO_7 still increases with decreasing temperature below 2.5 K (Fig. 7(a), upper figure).

3.2.5. Eu_3MoO_7

Fig. 8(a) shows the temperature dependence of the magnetic susceptibility for Eu_3MoO_7 in the temperature range of $1.8\,K < T < 400\,K$. No magnetic anomaly has been observed. Except at very low temperatures, the shape of this susceptibility vs. temperature curve is characteristic of Van Vleck paramagnetism, with a constant susceptibility for the lower temperature range and a decreasing susceptibility with increasing temperature for $T > 50\,K$. At very low temperatures ($T < 10\,K$), the magnetic susceptibilities suddenly increase with decreasing temperature. This magnetic behavior may be due to the properties of paramagnetic Mo^{5+} ions in Eu_3MoO_7. Fig. 8(b) depicts the specific heat vs. temperature curve for Eu_3MoO_7 below 15 K, showing no anomaly even in this low temperature range.

3.3. Structural phase transition

In order to ascertain the existence of structural phase transition in these Ln_3MoO_7, we have performed the DSC measurements for all compounds. Fig. 9 shows the DSC data for Ln_3MoO_7 (Ln = La, Pr, Nd, Sm, and Eu) in the temperature range of 350–800 K. For any Ln_3MoO_7 compound, two endothermic peaks in the DSC data were observed during heating, for example, at 371 and 484 K for La_3MoO_7, at 381 and 522 K for Pr_3MoO_7, and at 428 and 579 K for Nd_3MoO_7. Both the phase transition temperatures become higher from Ln = La to Eu.

Fig. 10 shows the temperature dependence of the lattice parameters for La_3MoO_7 in the temperature range of $300 < T < 500\,K$. The lattice parameters were refined with space group $P2_12_12_1$ for any temperature. With increasing temperature, the lattice parameter c increases monotonically, while the drastic changes have been observed at ca. 350 and 450 K for the parameter a, and at ca. 450 K for the parameter b. These temperatures are corresponding to the temperatures at which DSC anomalies have been observed (see Fig. 9(a)), i.e., the anomalies observed in the DSC measurements are due to the crystal phase transition.

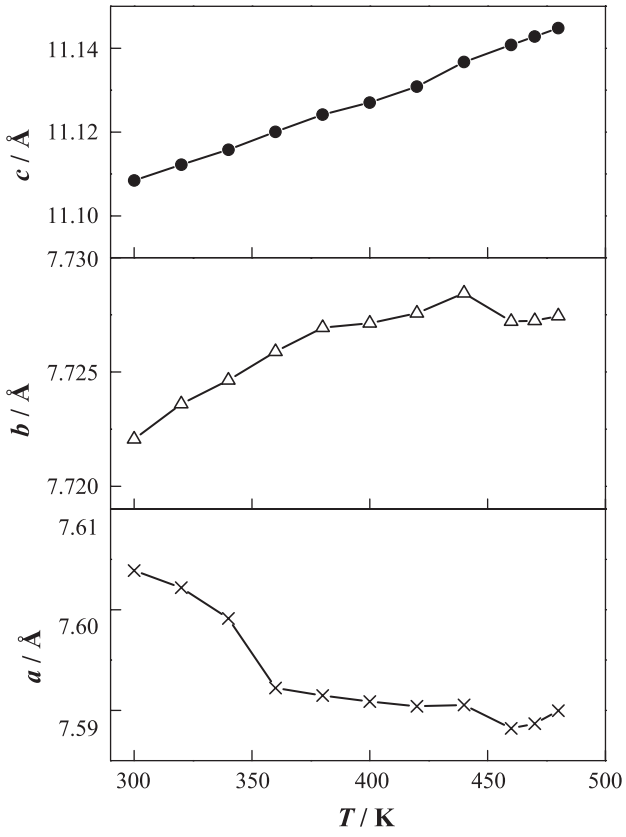

Fig. 10. Temperature dependence of lattice parameters for La_3MoO_7.

4. Summary

Ternary lanthanide–molybdenum oxides Ln_3MoO_7 (Ln = La, Pr, Nd, Sm, Eu) have been prepared and their magnetic properties have been characterized through magnetic susceptibility and specific heat measurements. La_3MoO_7 shows complex magnetic behavior at 150 and 380 K. Nd_3MoO_7 shows a clear antiferromagnetic transition at 2.5 K. Pr_3MoO_7 and Sm_3MoO_7 indicate the existence of magnetic anomaly at 8.0 and 2.5 K, respectively. The DSC measurements indicate that two phase-transitions occur for all Ln_3MoO_7 compounds in the temperature range between 370 and 710 K.

References

[1] J.G. Allpress, H.J. Rossell, J. Solid State Chem. 27 (1979) 105.
[2] H.J. Rossell, J. Solid State Chem. 27 (1979) 115.
[3] F.P.F. van Berkel, D.J.W. IJdo, Mater. Res. Bull. 21 (1986) 1103.
[4] W.A. Groen, F.P.F. van Berkel, D.J.W. IJdo, Acta Crystallogr. Sec. C 43 (1986) 2262.
[5] H. Prevost-Czeskleba, J. Less-Common Metals 127 (1987) 117.
[6] J.F. Vente, D.J.W. IJdo, Mater. Res. Bull. 26 (1991) 1255.
[7] A. Kahn-Harari, L. Mazerrolles, D. Michel, F. Robert, J. Solid State Chem. 116 (1995) 103.
[8] G. Wltschek, H. Paulus, I. Svoboda, H. Ehrenberg, H. Fuess, J.Solid State Chem. 125 (1996) 1.
[9] J.E. Greedan, N.P. Raju, A. Wegner, P. Gougeon, J. Padiou, J. Solid State Chem. 129 (1997) 320.
[10] P. Khalifah, R.W. Erwin, J.W. Lynn, Q. Huang, B. Batlogg, R.J. Cava, Phys. Rev. B 60 (1999) 9573.
[11] P. Khalifah, Q. Huang, J.W. Lynn, R.W. Erwin, R.J. Cava, Mater. Res. Bull. 35 (2000) 1.
[12] F. Wiss, N.P. Raju, A.S. Wills, J.E. Greedan, Inter. J. Inorg. Mater. 2 (2000) 53.
[13] B.P. Bontchev, A.J. Jacobson, M.M. Gospodinov, V. Skumryev, V.N. Popov, B. Lorenz, R.L. Meng, A.P. Litvinchuk, M.N. Iliev, Phys. Rev. B 62 (2000) 12235.
[14] D. Harada, Y. Hinatsu, J. Solid State Chem. 158 (2001) 245.
[15] D. Harada, Y. Hinatsu, J. Phys.: Condens. Matter 13 (2001) 10825.
[16] D. Harada, Y. Hinatsu, J. Solid State Chem. 164 (2002) 163.
[17] R. Lam, F. Wiss, J.E. Greedan, J. Solid State Chem. 167 (2002) 182.
[18] J.R. Plaisier, R.D. Drost, P.J.W. IJdo, J. Solid State Chem. 169 (2002) 189.
[19] R. Lam, T. Langet, J.E. Greedan, J. Solid State Chem. 171 (2003) 317.
[20] N. Barrier, P. Gougeon, Acta Crystallogr. E 59 (2003) i22.
[21] H. Nishimine, M. Wakeshima, Y. Hinatsu, J. Solid State Chem. 177 (2004) 739.
[22] M. Wakeshima, H. Nishimine, Y. Hinatsu, J. Phys.: Condens. Matter 16 (2004) 4103.
[23] Y. Hinatau, M. Wakeshima, N. Kawabuchi, N. Taira, J. Alloys Comp. 374 (2004) 79.
[24] F. Izumi, T. Ikeda, Mater. Sci. Forum 198 (2000) 321.
[25] R.L. Carlin, Magnetochemistry, Springer, New York, 1986.